Electrochemical and Spectroelectrochemical Investigations of "Figure-Eight" Octapyrrolic Macrocycles, Free Bases, and Their Mononuclear, Homo- and Heterodinuclear Complexes with Divalent Transition Metals

Jordi Bley-Escrich,[a] Jean-Paul Gisselbrecht,[a] Emanuel Vogel,[b] and Maurice Gross*[a]

Keywords: Macrocyclic ligands / Octaphyrins / Transition metal complexes / Electrochemistry

This work reports on electrochemical investigations of "figure-eight"-shaped cyclooctapyrrolic macrocycles (octaphyrins) **1**–**3** and of some of their mono- and dinuclear transition metal complexes. The octaphyrins **1**–**3** differ mainly in the size of the main conjugation pathway, which involves either $4n$ π-electrons for **1** and **3**, or $(4n + 2)$ π-electrons for **2**. All species studied undergo six redox steps, namely two reductions and four oxidations. The two reductions and the first three oxidations are reversible one-electron transfers. The fourth oxidation is either reversible, or irreversible due to a subsequent chemical reaction. Depending on the complex studied, the third and fourth oxidations occur either at similar potentials, so that a global two-electron step is observed, or at distinct potentials, leading to two well-separated signals. Spectroelectrochemical investigations demonstrate that all redox processes are ligand centred. The reported results clearly indicate that the redox potential changes in these new octapyrrolic macrocycles depend much more on structural contributions, due to their figure-eight topography, than on characteristics such as ionic radius or electronegativity of the coordinated metal. The HOMO-LUMO gap in the series of octaphyrins studied is rather small (about 1 eV), and is not only related to the macrocyclic ring size, but also depends on whether the main conjugation pathway involves $4n$ or $(4n + 2)$ π-electrons.

Introduction

Expanded porphyrinoids with five or more conjugated pyrrolic rings have attracted interest since the discovery of the pentapyrrolic sapphyrin by Woodward, Dolphin, and Johnson.[1−3] Subsequent to this early work, various cyclopolypyrroles, namely penta- and hexapyrrolic ring systems[4−8] have been prepared and identified. More recently, a new cyclodecapyrrole called turcasarin,[9] and a family of cyclooctapyrroles, named octaphyrins,[10−12] belonging to figure-eight-shaped cyclopolypyrroles have been obtained. Giant cycles containing up to 16 pyrrole units have also been synthesised and identified very recently.[13−15]

Despite this very large set of polypyrrolic macrocycles now available, the complexing abilities of these new expanded macrocycles have only been investigated for a few compounds,[16] and electrochemical studies remain scarce.[17]

The cyclooctapyrroles (COP) presently known,[10−12] i.e., **1** {[32]COP(1.0.1.0.1.0.1.0)},[18] **2** {[34]COP(1.1.1.0.1.1.1.0)},[18] and **3** {[36]COP(2.1.0.1.2.1.0.1)}[18] (all three series studied in this publication), are employed as hexadecaethyl derivatives (Figure 1) for reasons of solubility. A characteristic feature of these cyclooctapyrroles is that they are folded in such a way so as to adopt figure-eight conformations with approximate D_2 symmetry, both in solution and in the solid state as confirmed by NMR spectroscopic studies and X-ray crystallographic analysis.[19−20] NMR spectroscopic studies of these cyclooctaphyrin free bases confirmed their nonaromatic character, whether they possess $(4n + 2)$ [**2** (34)] or $4n$ [**1** (32) and **3** (36)] π-electrons in their main conjugation pathway. The figure-eight-shaped structure of cyclooctaphyrins provides two equivalent porphyrin-sized cavities for metal complexation, enabling the generation of mononuclear, homodinuclear and heterodinuclear complexes. However, depending on the ring size, all three types of complexes could be prepared with **1** and **2**. On the other hand, only homodinuclear complexes could be obtained and identified with ligand **3**.[21]

Until now, electrochemical investigations of macrocyclic polypyrroles containing more than four pyrrole units remain rather scarce,[17] and studies on octapyrrolic macrocycles are restricted to preliminary studies on the free bases and some complexes of **1** and **3** in CH_2Cl_2.[22] In the present paper the electrochemical behaviour of a new series of cyclooctaphyrins, namely **2**, has been investigated in dry benzonitrile. Its behaviour will be compared with previously

[a] Laboratoire d'Electrochimie et de Chimie Physique du Corps Solide, UMR 7512 − CNRS Université Louis Pasteur, 4, rue Blaise Pascal, 67000 Strasbourg, France
Fax: (internat.) + 33-3/90241431
E-mail: gross@chimie.u-strasbg.fr
[b] Institut für Organische Chemie, Universität zu Köln, Greinstrasse 4, 50939 Köln, Germany

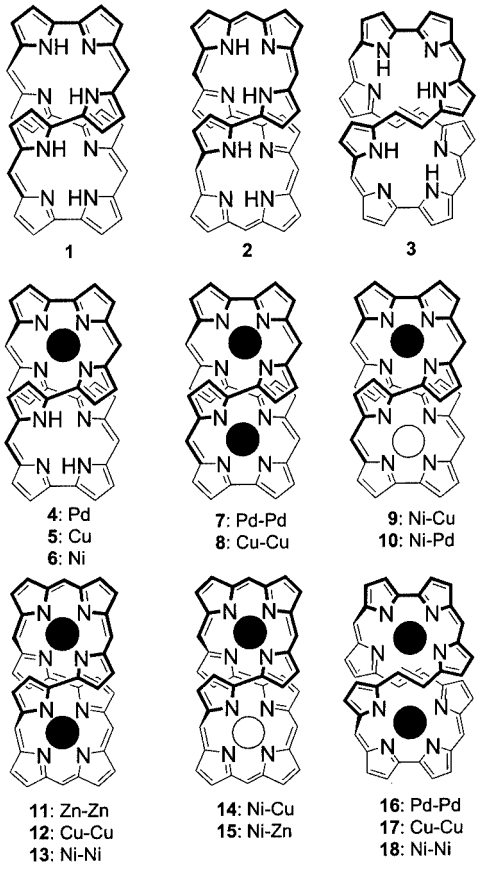

Figure 1. Free bases and complexes, studied in the three hexadecaethylcyclooctaphyrin series; the ethyl groups are omitted for clarity

published data[22] involving **1** and **3**. However, to obtain a better insight into the redox behaviour of the three series of COP and to allow consistent comparison, the previously studied COP (**1**, **3**−**10**, **16**−**18**) have been reinvestigated here in dry benzonitrile by hydrodynamic voltammetry, by cyclic voltammetry, and by UV/Vis spectroelectrochemistry.

Results and Discussion

Results

In order to obtain useful information on the redox properties of the cyclooctaphyrins **1**, **2**, and **3** and their complexes (Figure 1), studies were carried out by cyclic voltammetry (CV) and hydrodynamic voltammetry on a platinum RDE in dry PhCN + 0.1 M Bu_4NPF_6 solutions at 25 °C on the three series of cyclooctaphyrins.

Hydrodynamic voltammetry of **1** and its complexes **4**−**10** show similar redox behaviour. Indeed, all species exhibit, as illustrated for the Pd−Pd complex **7** (Figure 2), two reduction waves of equal amplitude, as well as three oxidation waves. The first two oxidation waves have the same limiting current as the reduction waves, whereas the current for the third oxidation is twice that of the previous steps. For the complexes **4**−**10**, this later wave is broader, depending on the complex studied. Wave analysis, using Tomeš criteria,[23] give slopes $|E_{3/4} - E_{1/4}|$ close to 56.4 mV for the two reductions and the first two oxidations, whereas the third oxidations have slopes ranging from 60 to 170 mV, depending on the coordinated metal ion(s). For the two reductions and the first two oxidations, the observed slopes are consistent with reversible one-electron exchanges, whereas the slope for the third oxidation, involving two electrons will be studied by CV to obtain more information on its electron transfer mechanism. The potentials obtained by hydrodynamic voltammetry are in agreement with those observed by CV, and they are reported in Table 1.

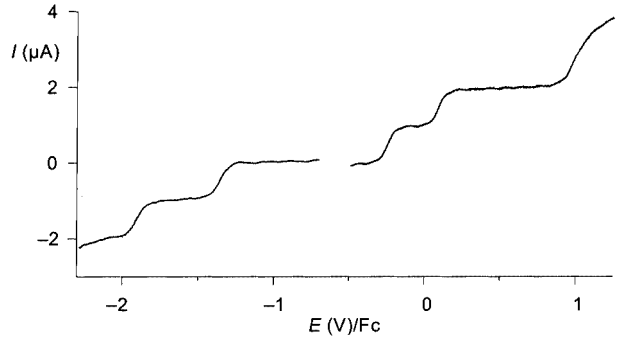

Figure 2. Hydrodynamic voltammetry of **7** in PhCN + 0.1 M Bu_4NPF_6, on Pt working electrode; scan rate: 0.01 V/s (potentials vs. Fc)

The CVs for **1** and its complexes are given in Figure 3 and their redox potentials are reported in Table 1. For the free base, as well as for the complexes studied, two one-electron reversible reductions are observed. For the oxidations, the first two electron transfers are also one-electron reversible oxidations, as confirmed by the monitoring of their peak current (I_p) and peak potentials (E_p) with scan rate. The corresponding peak potentials are constant with scan rates of up to 5 V/s, the peak current ratio I_{pa}/I_{pc} is close to unity at any v, the peak potential difference $\Delta E = E_{pc} - E_{pa}$ is approximately 60 mV up to 5 V/s, and a linear correlation intercepting the origin is observed by plotting I_p vs. $v^{1/2}$.

Further oxidation steps deserve specific comments. The free base **1** and the mononuclear complexes **4**−**6** exhibit a third oxidation step, which is irreversible at scan rates lower than 1 V/s. At scan rates higher than 1 V/s, this third step becomes reversible for complexes **4**−**6**, and reversible only at scan rates higher than 5 V/s for **1**. Analysis of the peak characteristics show that the plot I_{pa} vs. $v^{1/2}$ is a straight line intercepting the origin for scan rates lower than 0.2 V/s. Its slope is twice that of the first and second oxidation, consistent with a two-electron transfer, as indicated from the results obtained in hydrodynamic voltammetry. At scan rates higher than 0.2 V/s, the peak current evolution was slightly curved to the x axis. In addition, the peak current ratio I_{pa}/I_{pc} increases with scan rate to unity. The peak shape ($E_p - E_{p/2}$) is specific to the species studied (45 mV for **1**, 100 mV for **4** and 60 mV for **5** at v = 0.1 V/s) and increases with scan rate. Although no clear conclusion

Table 1. Redox potentials obtained by cyclic voltammetry, in PhCN + 0.1 M Bu_4NPF_6, on Pt working electrode; scan rate: 0.1 V/s; $E = (E_{pc} + E_{pa})/2$ (potentials vs. Fc)

COP(1.0.1.0.1.01.0)	$Ered_2$ [V]	$Ered_1$ [V]	Eox_1 [V]	Eox_2 [V]	Eox_3 [V]	Eox_4 [V]	$Eox_1 - Ered_1$ [V]
H_4COP (**1**)	−2.02	−1.64	−0.18	0.08	1.01[a]	1.06[a]	1.46
PdH_2COP (**4**)	−1.91	−1.42	−0.20	0.16	0.99[b]	1.07[b]	1.22
CuH_2COP (**5**)	−2.06	−1.30	−0.26	0.10	1.05[b]	1.09[b]	1.04
NiH_2COP (**6**)	−1.96	−1.44	−0.27	0.10	0.95	1.08	1.17
Pd_2COP (**7**)	−1.93	−1.38	−0.27	0.07	0.87	0.91	1.11
Cu_2COP (**8**)	−2.07	−1.29	−0.39	0.00	0.97	1.01	0.90
NiCuCOP (**9**)	−2.00	−1.26	−0.33	0.04	0.91	0.95	0.93
NiPdCOP (**10**)	−1.90	−1.34	−0.26	−0.02	0.95	0.99	1.08
COP(1.1.1.0.1.1.1.0)	$Ered_2$ [V]	$Ered_1$ [V]	Eox_1 [V]	Eox_2 [V]	Eox_3 [V]	Eox_4 [V]	$Eox_1 - Ered_1$ [V]
H_4COP (**2**)	−1.88	−1.40	−0.30	0.13	0.83	1.21	1.10
Zn_2COP (**11**)	−1.89	−1.38	−0.35	0.09	0.78	1.01	1.03
Cu_2COP (**12**)	−1.92	−1.37	−0.36	0.13	0.80	1.03	1.01
Ni_2COP (**13**)	−1.87	−1.35	−0.37	0.11	0.72	0.76	0.98
NiCuCOP (**14**)	−1.89	−1.36	−0.36	0.12	0.76	0.80	1.00
NiZnCOP (**15**)	−1.88	−1.37	−0.35	0.11	0.72	0.76	1.02
COP(2.1.0.1.2.1.0.1)	$Ered_2$ [V]	$Ered_1$ [V]	Eox_1 [V]	Eox_2 [V]	Eox_3 [V]	Eox_4 [V]	$Eox_1 - Ered_1$ [V]
H_4COP (**3**)	−1.68	−1.37	−0.15	0.08	0.89[c]	0.93[c]	1.22
Pd_2COP (**16**)	−1.58	−1.18	−0.25	0.09	0.78	0.82	0.93
Cu_2COP (**17**)	−1.69	−1.18	−0.38	−0.08	0.69	0.73	0.80
Ni_2COP (**18**)	−1.64	−1.22	−0.32	0.08	0.55	0.59	0.90

[a] Reversible above scan rate 5 V/s. [b] Reversible above scan rate 1 V/s. [c] Reversible above scan rate 0.5 V/s.

could be drawn from these data from known criteria,[24] these results are fully consistent with a third oxidation obeying an $E_{rev}E_{rev}C_{irr}$ mechanism. Such a mechanism is indeed observed for complex **6** (belonging to the same series of species studied), with distinct potentials for both steps. Actually, the NiH_2 complex **6** undergoes distinct third and fourth one-electron oxidations. Reversing the scan after the third oxidation confirms the reversibility of the third oxidation, whereas the fourth oxidation remains irreversible at scan rates lower than 1 V/s. Digital simulation using DIGISIM software[25] confirms the proposed mechanism, as illustrated for **1** in Figure 4, and allows us to access to the corresponding potentials. The final species generated could not be identified. However, the species generated is electroactive and could be identified by its reduction around +0.7 V/Fc on the reverse scan.

The complexes **7**−**10** exhibit a two-electron, reversible third oxidation at all scan rates. The redox potentials are presented in Table 1. For this third step, wave analysis gives slopes close to 60 mV in hydrodynamic voltammetry, and the peak potential difference $\Delta E_p = E_{pa} - E_{pc}$ is close to 60 mV up to 1 V/s. These characteristics are in agreement with two overlapping reversible one-electron transfers, whose redox potentials are separated by 35.6 mV, as predicted by Savéant[26] for hydrodynamic voltammetry and Shain[27] for CV. The latter transfers occur at two independent redox centres whose potentials are given in Table 1.

For **2** and its homo- and heterodinuclear complexes **11**−**15**, the redox behaviour is similar to the results reported above. All these species undergo two one-electron reversible reductions. Oxidation of the free base **2** gives four well-separated one-electron reversible steps, whereas for complexes **11** and **12** the fourth oxidation is irreversible as shown by CV (Figure 5). Oxidation of **13**, **14** and **15** occurs in three steps, the first two are one-electron reversible oxidations, and the third step is a reversible two-electron step. Analysis of the peak characteristics indicate that the third oxidation involves two reversible overlapping one-electron steps whose potentials are reported in Table 1.

Ligand **3** and its homodinuclear complexes **16**−**18** all have similar redox behaviour, namely two one-electron reduction steps, as well as three oxidations as shown in Figure 6. The first two oxidations are reversible one-electron transfers, whereas the third oxidation has the characteristics of two overlapping one-electron reversible transfers. Indeed, wave analysis of the third oxidation step gives a slope close to 60 mV by hydrodynamic voltammetry, whereas the peak potential difference in CV, $E_{pc} - E_{pa}$, is approximately 60 mV at scan rates up to 1 V/s. As two electrons are involved in the third step, these characteristics are in agreement with two one-electron transfers separated by 35.6 mV,[26,27] which occur at two independent redox centres. In order to identify the electron-transfer sites, spectroelectrochemical studies have also been carried out.

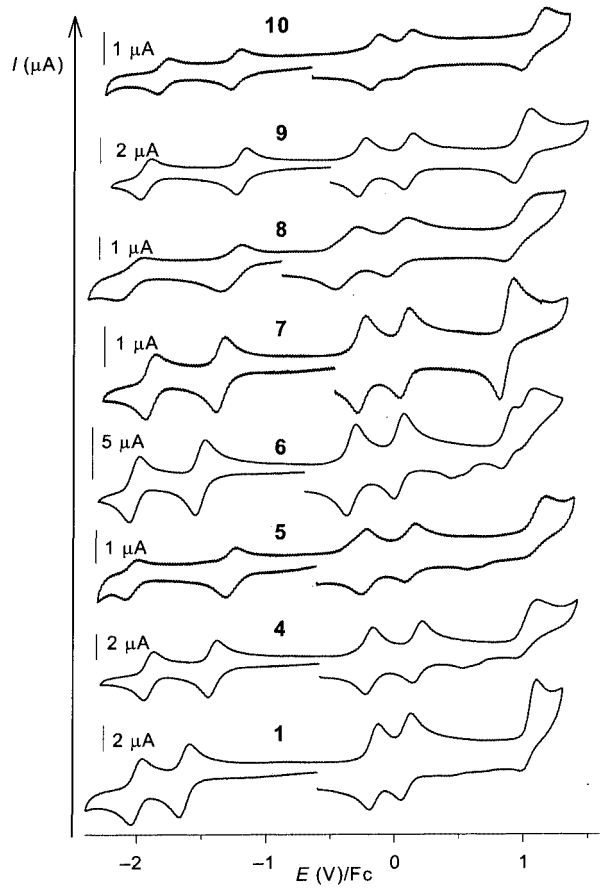

Figure 3. Cyclic voltammetry of **1** and **4**−**10** in PhCN + 0.1 M Bu_4NPF_6, on Pt working electrode; potential vs. Fc; scan rate: 1 V/s for **1** and 0.2 V/s for **4**−**10**

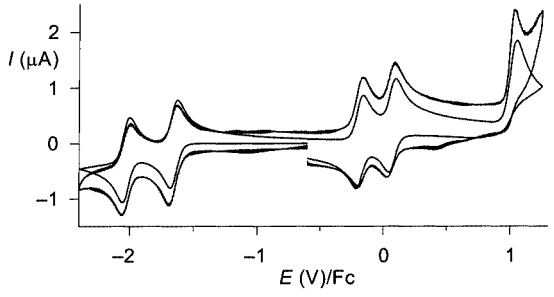

Figure 4. Cyclic voltammetry of **1** (solid line) in PhCN + 0.1 M Bu_4NPF_6, on Pt working electrode (scan rate: 0.1 V/s) and simulation using the software DIGISIM[25] (dashed line) for an oxidation mechanism involving four subsequent one electron oxidations at distinct potentials (E_1−E_4), the fourth step is followed by an irreversible chemical reaction (C_{irr}); the global reaction scheme may be the represented as $E_1E_2E_3E_4C_{irr}$; parameters used for oxidation: $E_1 = -0.18$ V ($k_s = 10^4$ cm/s); $E_2 = +0.08$ V ($k_s = 10^4$ cm/s); $E_3 = +1.01$ V ($k_s = 0.01$ cm/s); $E_4 = +1.06$ V ($k_s = 0.01$ cm/s) and for the chemical reaction: $Ox_4 \rightarrow X$, the equilibrium constant was $K_{eq} = (k_f/k_b) = 1000$; parameters used for reduction: $E_1' = -1.65$ V ($k_s = 10^4$ cm/s); $E_2' = -2.02$ V ($k_s = 10^4$ cm/s) (potentials vs. Fc)

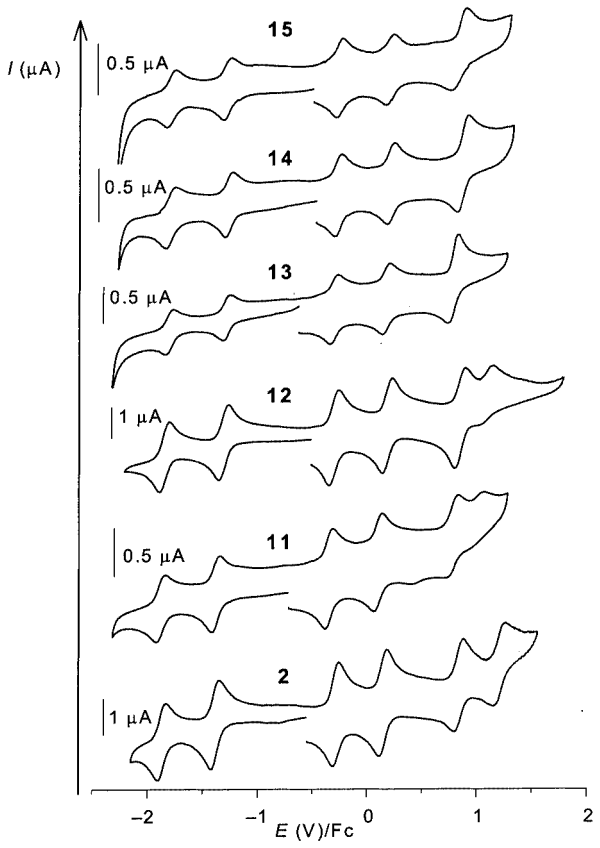

Figure 5. Cyclic voltammetry of **2** and **11**−**15** in PhCN + 0.1 M Bu_4NPF_6, on Pt working electrode; scan rate: 0.05 V/s (potentials vs. Fc)

Spectroelectrochemistry

Spectroelectrochemistry was carried out on each compound. The spectra showing the two reduction steps and the four oxidations exhibit, in general, well-defined isosbestic points. During the two reductions and the first two oxidations, the species generated exhibit specific absorbance bands. The initial spectrum could be recovered quantitatively by stepwise electrochemical restoration of the initial cyclooctaphyrin. This indicates that the two electroreduced and the two electrooxidised species are chemically stable on the time scale of the spectroelectrochemical experiments, i.e. about 30 min, a good indication of the high stability of the electrogenerated species under the experimental conditions.

In general, the third and fourth oxidations do not revert to the initial spectrum after spectroelectrochemical measurements, due to the chemical reaction coupled to the fourth oxidation step, hence leading to global irreversibility. When the third and fourth oxidations occur at quite distinct potentials (i.e. for the Zn_2 and Cu_2 complexes **11** and **12**), allowing for the trioxidised and the tetraoxidised species to be obtained separately, the trioxidised species quantitatively reverts to the initial spectrum by stepwise electrochemical restoration of the initial species.

The spectral changes during electrolysis are similar for **1** and its complexes **4**−**10**, as well as for **3** and its complexes **16**−**18**. Therefore, the behaviour of one representative compound, Pd_2 complex **16**, will be described for these two series (**a**, **b** in Figure 7). The neutral species presents a main absorbance band at 660 nm, and no bands are detected

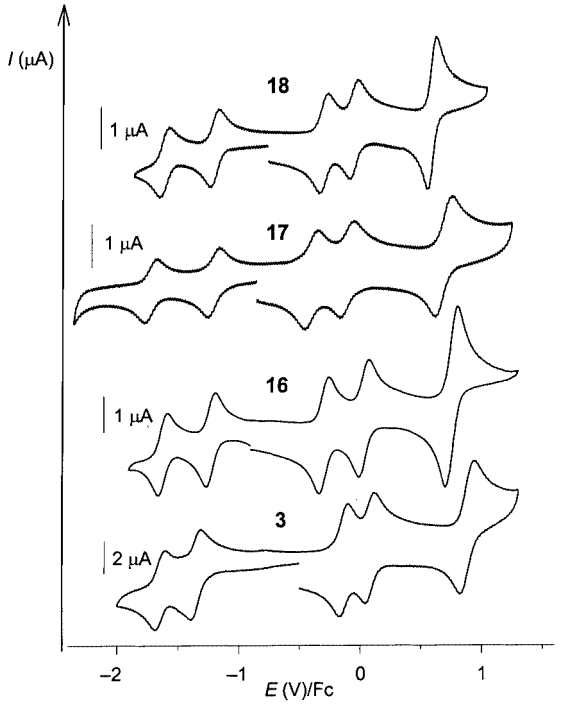

Figure 6. Cyclic voltammetry of **3** and **16**−**18** in PhCN + 0.1 M Bu_4NPF_6, on Pt working electrode; scan rate: 1 V/s for **3** and 0.2 V/s for **16**−**18** (potentials vs. Fc)

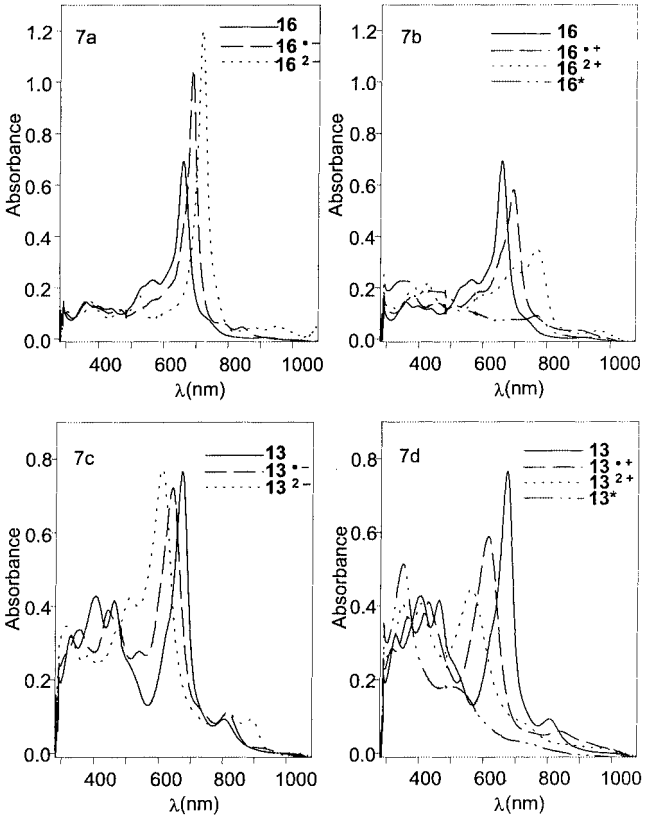

Figure 7. Spectroelectrochemistry of COP **16** and **13**, in PhCN + 0.1 M Bu_4NPF_6; reductions (see **a**) and oxidations (see **b**) of **16**; reductions (see **c**) and oxidations (see **d**) of **13**; *: spectrum corresponding to the species resulting from the irreversible chemical reaction following the fourth oxidation

from 800 to 1100 nm. During electrolysis on the plateau potential corresponding to the first reduction, the main band shifts to the red (691 nm) and its intensity increases by 75%, while some small bands appear between 800 and 900 nm. The main band shifts to a lower energy (720 nm) and its intensity increases again by 20%, after further electrolysis at the potential of the second reduction. Small bands appear between 900 and 1000 nm and an absorbance band is detected at 1078 nm. Spectra of the neutral, mono- and di-reduced species are presented in Figure 7 (see **a**). For the oxidation, the behaviour is quite similar for the first and second steps: the main absorbance band undergoes a red shift during the first oxidation electrolysis (696 nm), while its intensity decreases relative to the intensity of the neutral compound. The electrolysis at the second oxidation potential leads to a spectrum in which the main absorbance band also undergoes a red shift (771 nm) and is less intense.

During the third oxidation step, the intensity of all bands beyond 550 nm decreases considerably, or the bands completely disappear. This step is not reversible on the time scale of spectroelectrochemistry. Spectra characterising the species generated during oxidative electrolysis are presented in Figure 7 (see **b**).

The spectroelectrochemical behaviour of **2** and its complexes **11**−**15** is similar to the results presented above. However, a blue shift of the main absorbance band is observed during reduction, as well as during oxidation, as illustrated in the case of complex **13** (see **c**, **d** in Figure 7). The most intense main absorbance band is observed in the neutral compound spectrum, and not for the di-reduced species as observed previously with **1**, **3**, and their respective complexes.

These redox and spectral characteristics unambiguously indicate that the metal complexes of the cyclooctaphyrins studied undergo redox processes very similar to those of the free bases. Comparison of these reduction and oxidation potentials of the free bases with those of their metal complexes, as well as the spectral modifications associated with electron transfer in each redox step, lead to the reasonable conclusion that the electron transfer processes occur on the cyclooctapyrrolic ligand in the free bases and also in the complexes studied.

Discussion

The present electrochemical investigations clearly demonstrate that all the free bases and complexes studied above undergo six one-electron transfers on the conjugated cyclooctapyrrolic ring, namely two well-separated reversible one-electron reduction and four oxidation steps. The first three oxidations are reversible one-electron steps, whereas the fourth oxidation is either reversible, in most cases, or is irreversible in the species **1**, **4**, **5**, **6**, **11**, and **12**. For almost all the species studied, the last two oxidations occur at fairly close potentials ($Eox_4 - Eox_3 = 35.6$ mV), giving, macroscopically, a unique two-electron transfer, except in **2**, **6**,

11, **12** where the third and fourth oxidation potentials are separated by more than 80 mV. The third oxidation step observed, involving two-electron transfers separated by 35.6 mV and corresponding to oxidations at almost independent redox centres, is not well understood for COP. It could either result from non-interacting redox centres in the ligand, or from geometric changes occurring after the third electron exchange, which raises the energy level of the HOMO, making the removal of the fourth electron easier.[28] Theoretical approaches should be undertaken in order to obtain a better insight into these new families of compounds. Nevertheless, it should be stressed that unlike other polypyrrolic macrocycles, such as porphyrins, the COP ligands studied here are not planar[19,20] and do not possess an aromatic π-electron system, although they are fully conjugated. Therefore, it is possible that the removal of two electrons from the same HOMO orbital, occurring at two distant sites in the ligand, avoiding any coulombic repulsion, occurs in a unique step. However, until further information is made available, conformational changes triggered by the third oxidation thus allowing for the removal of the fourth electron at the same potential may not be ruled out, since geometric and steric factors contribute to the electrochemical behaviour, as pointed out hereafter.

Comparison of the redox potentials lead to interesting observations. Disregarding the species involving **3**, for which the number of complexes studied is too small (free base **3** and complexes **16**−**18**) to allow significant comparisons, it may be observed from Table 1 that **2** and its complexes **11**−**15**, possessing ($4n$ + 2) π-electrons in the main conjugation pathway, present very close mean reduction potentials values ($E\text{red}_1$ = −1.36±0.04 V, $E\text{red}_2$ = −1.89±0.03 V/Fc). In contrast, **1** and its complexes **4**−**10**, possessing $4n$ π-electrons, present a greater spread in their mean reduction potentials values ($E\text{red}_1$ = −1.35±0.09 V, $E\text{red}_2$ = −1.98±0.08 V/Fc). However, the difference between these two values remain similar for **2** and its complexes ($E\text{red}_1 - E\text{red}_2$ = +0.52±0.03 V) and for **1** and its complexes ($E\text{red}_1 - E\text{red}_2$ = +0.53±0.03 V), except for the complexes of **1** that contain copper (0.75 V). The similarity in these values is a good indication that all the reductions occur on the ligand, and they are also consistent with the possible explanation that the potential difference corresponds to the energy repulsion between two electrons filling the same orbital.[29]

The same conclusions are observed for the oxidation processes. For **2** and its complexes, the first two oxidation potentials are quite similar ($E\text{ox}_1$ = −0.37±0.02 V, $E\text{ox}_2$ = +0.10±0.03 V), whereas **1** and its complexes present more dispersed mean potential values ($E\text{ox}_1$ = −0.29±0.09 V, $E\text{ox}_2$ = +0.06±0.10 V). The potential difference between the first and second oxidations in each series are also quite similar. Indeed $E\text{ox}_1 - E\text{ox}_2$ = +0.46±0.03 V for **2** and its complexes, and $E\text{ox}_1 - E\text{ox}_2$ = +0.36±0.03 V for **1** and its complexes, except for **10** (0.24 V). As observed recently by Guyard et al.,[30] who studied the oxidation behaviour of several pyrrole oligomers, namely pyrrole to tetrapyrrole, the longer the chain, the easier the oxidations. The tetrapyrrole was easily oxidised (stepwise) at −0.16 and +0.12V/Fc like COP. The low potentials associated with the first two oxidations of COP agree with those results, assuming that COP behave like polypyrroles, independent of their cyclic or conjugation characteristics. It has to be mentioned that in the present set of cyclooctaphyrins studied, no correlation between the observed redox potentials and the electronegativity of the complexed metals could be established, in contrast with results observed with porphyrins or porphyrin isomers.[31−33] This suggests that geometric and steric factors contribute in good part to the electrochemical behaviour of COP.

In a given set of molecules, advantage may be taken from the existing correlation between the energy of the HOMO orbital and at least the first oxidation potential, and also between the LUMO and the first reduction potential. In such a case the difference $E\text{ox}_1 - E\text{red}_1$ may be taken as a good approximation of the energy gap between the HOMO and the LUMO orbitals.[32,34] The energy gaps for cyclooctaphyrins are relatively low (Table 1), compared with aromatic polypyrrolic macrocycles like porphyrins (2.25±0.15 V)[32] or porphycenes (1.85±0.15 V),[33,35−37] but they are similar to that of expanded porphycenes containing 26 π-electrons (1.01 V).[38] This low energy gap observed in cyclooctaphyrins is therefore related to the extension of the π-conjugation pathway. However, as observed in free bases **1**−**3**, the gap does not decrease on increasing the size of the conjugated macrocycle. Indeed, the highest value belongs to the smallest cyclooctaphyrin **1** (ΔE = 1.46 V), followed by the largest macrocycle **3** (ΔE = 1.22 V), and finally the smallest gap corresponds to the middle-sized cyclooctaphyrin **2** (ΔE = 1.10 V). These values are in agreement with the observed lowest energy bands observed in CH_2Cl_2, as shown in Figure 8. Indeed, **2** gives well-defined bands, the less energetic band being located at 1280 nm (0.97 eV). In contrast, both free-bases **1** and **3** only exhibit small amplitude absorbance bands at 865 (1.43 eV) and 932 nm (1.33 eV), respectively. However, this is parallel to the energy sequence of the most intense bands in the UV/Vis spectra of these macrocycles (λ = 534 nm for **1**, λ = 596 nm for **3**, and λ = 660 nm for **2**), illustrated in Figure 8.

For the species studied (Figure 9), **2**, **11**−**15** [($4n$ + 2) π-electrons] exhibit an almost constant gap within the series of the five complexes studied (ΔE =1.00±0.10 V). In complexes of **1** and **3** ($4n$ π-electrons), this difference decreases drastically from the free base to mononuclear complexes, and further to dinuclear complexes (Figure 9). For example, in mononuclear complexes **4**−**6** these values change drastically in the series, the highest belonging to **4** and the lowest to **5**. These variations could not successfully be correlated to any metal characteristics (electronegativity, ionization potential, ionic radius, ...), and therefore we are inclined to conclude that this evolution is basically related to geometric and steric parameters characterising the cations in the cavity of cyclooctaphyrins.

The results obtained from spectroelectrochemical studies on cyclooctaphyrins confirm that all redox steps occur on the ligand, and that no metal-centred transfer is observed

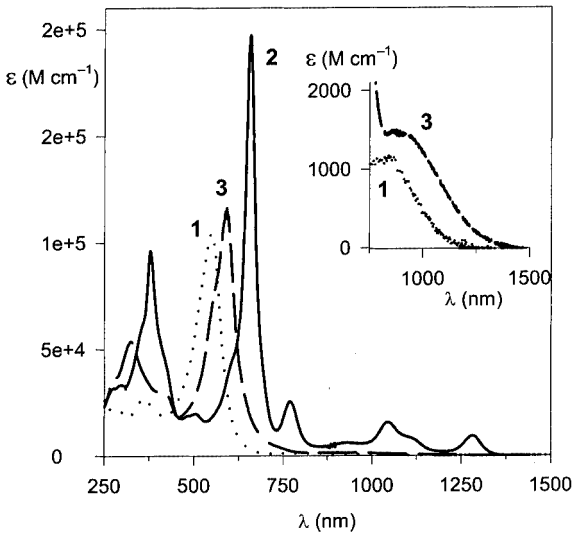

Figure 8. UV/Vis absorbance spectra of the three free bases **1**, **2**, and **3**, in CH_2Cl_2

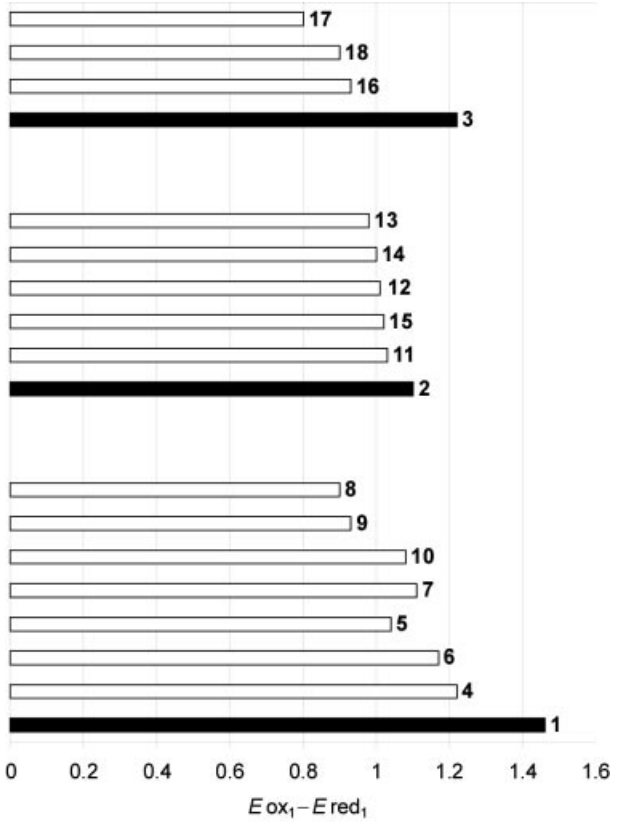

Figure 9. Potential difference $E\text{ox}_1 - E\text{red}_1$ [V], estimation of the HOMO−LUMO gap, for the three cyclooctaphyrin series

in the series studied. Some unexpected trends within the three series of compounds studied are observed. Indeed, although none of the species studied involves an aromatic ligand (even though they have 34 or 38 π-electrons [(4*n* + 2) π-electrons]),[11,39] the observed spectra obtained from spectroelectrochemistry are markedly different, depending on whether the ligands possess 4*n* or (4*n* + 2) π-electrons.

Such unexpected spectral changes are documented from comparison among the three COP families, more specifically when comparing the families with 4*n* π-electrons with the family with (4*n* + 2) π-electrons. Indeed, the spectra of the families with 4*n* π-electrons show a red shift during the two reductions and the first two oxidations, both corresponding to changes from 4*n* to (4*n* + 2) π-electrons. More explicitly, the species with (4*n* + 2) π-electrons exhibit a narrow and intense band whose wavelength depends on the family studied: this absorbance band is located close to 660 nm for the neutral species **2** and its complexes, and close to 725 nm for the di-reduced species **1**, **3**, and their complexes. The intensity and the geometry of this band is reminiscent of the characteristics of a Soret band, although the species are not aromatic.[11,39] On the contrary, the spectra of the family initially possessing (4*n* + 2) π-electrons shifts to the blue during the reductions and the oxidations, i.e. when changing from (4*n* + 2) to 4*n* π-electrons. Based on such related 4*n* or (4*n* + 2) π-electron numbers, the two evolutions are consistent. Another interesting observation was carried out for cyclooctaphyrins containing (4*n* + 2) π-electrons, including di-reduced **1** and **3**, as well as the neutral ligands **2**, and their respective metal complexes: all exhibit a particular similarity in their UV/Vis absorbance spectra. On the contrary, the absorbance band wavelength of the species having 4*n* π-electrons in their main conjugation pathway depends to a large extent on the chemical nature of the complexed metal(s).

The presence of this intense and sharp band in the species possessing (4*n* + 2) π-electrons is surprising for these macrocycles, in particular because of their twisted ("figure-eight") conformation. Still more surprising is the observation that the absorbance bands of the neutral ligand **2** and its complexes and those of the di-reduced species **3** and its complexes are perfectly located on the linear correlation (established previously by Franck et al. for aromatic planar expanded porphyrins)[40] between the wavelength of the Soret-like band and the number of conjugated π-electrons belonging to expanded macrocycles, named Babuška Porphyrins.

In the absence of any study or review available on macrocyclic polypyrroles analysing their spectral evolution with the size of the conjugated macrocycles, we plotted the wavelength of the most intense band of known polypyrrolic macrocycles, versus the number of π-electrons in the main conjugation pathway. The data collected, shown in Figure 10, involve species containing (4*n* + 2) π-electrons as well as 4*n* π electrons, their conformation being either planar or twisted "figure-eight". Two linear correlations are obtained (Figure 10) for species with (4*n* + 2) and with 4*n* π-electrons, respectively. These two correlations differ in their slopes. A greater slope is obtained for the correlation involving macrocycles with (4*n* + 2) π-electrons. Both correlations intercept at a common point, which has no physical meaning. Such correlations were never reported previously on polypyrrolic macrocycles. However, the same kind of

correlation has been established by Märkl et al.[41] for tetraoxaporphyrins, possessing (4*n* + 2) π-electrons, and also for tetraepoxyannulenes with 4*n* π-electrons. The two correlations were linear and differed mainly in their slopes. It has to be mentioned here that the two linear correlations with macrocycles involving (4*n* + 2) π-electrons containing either N or O heteroatoms overlap, whereas for macrocycles containing 4*n* π-electrons the two correlations possess similar slopes, but with different ordinates (the wavelength of the macrocycles with O heteroatoms is blue-shifted relative to the polypyrrolic macrocycles).[41]

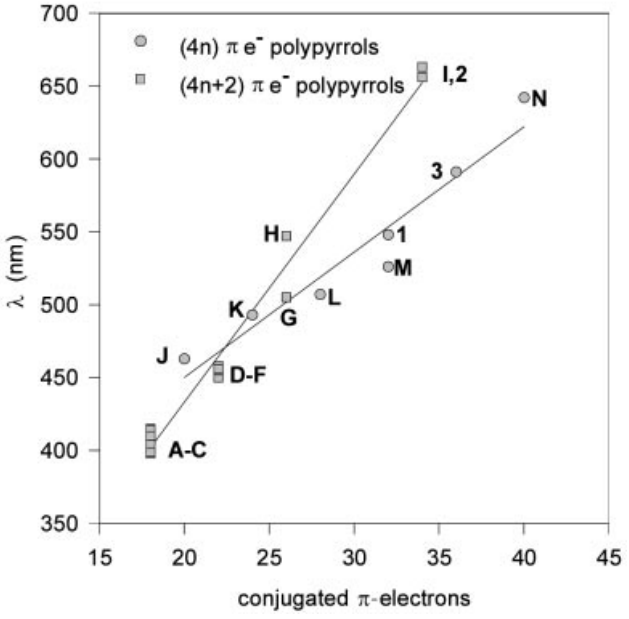

Figure 10. Correlation established for the main absorbance bands in UV/Vis spectra of polypyrrolic macrocycles versus the number of π-electrons involved in the main conjugation pathway; **A**: porphyrin;[40,42] **B**: corrphycene;[43,44] **C**: hemiporphycene;[45,46] **D**: sapphyrin;[3,42,47,48] **E**: pentaphyrin;[4] **F**: smaragdyrine;[49] **G**: rubyrine;[7] **H**: (3.3.3.3)porphyrin;[40] **I**: (5.5.5.5)porphyrin;[40] **J**: orangarin;[50] **K**: amethyrin;[50] **L**: heptaphyrin;[12] **M**: octaphyrin(1.0.0.0.1.0.0.0);[12] **N**: turcasarin;[9] **1**;[10] **2**;[11] **3**[11]

The observed correlations (Figure 10) with two different slopes rationalise the results of the spectroelectrochemical experiments. As reported above, the spectra from cyclooctaphyrins possessing 4*n* π-electrons undergo a red shift after two one-electron reductions, generating (4*n* + 2) π-electron species. Spectral evolutions for cyclooctaphyrins with (4*n* + 2) π-electrons undergo a blue shift under the same conditions, which is in agreement with the observed evolutions given in Figure 10, above the intercept.

The data reported above and correlations clearly indicate that the polypyrrolic macrocycles containing (4*n* + 2) π-electrons exhibit greater homogeneous characteristics. For instance, the redox potentials of **2** and its complexes **11**−**15** are identical, and the observed HOMO−LUMO gap is very similar for the series. Also their UV/Vis spectra give strong Soret-like bands at similar wavelengths. The homogeneity of such data for macrocycles containing (4*n* + 2) π-electrons most likely results from a stabilised structure, due to the presence of (4*n* + 2) π-electrons in cyclooctaphyrins. From the spectroelectrochemical studies, the dianion of **1**, **3**, and of their complexes also exhibit well-resolved sharp bands located at 725 nm.

Conclusion

The studied cyclooctaphyrins undergo six redox steps, two one-electron reversible reductions and four one-electron oxidations, the first three oxidations are one-electron reversible transfers. For some derivatives, the fourth oxidation is irreversible. The potential difference between the third and fourth oxidation is rather small in most of the species studied (close to 40 mV), resulting in a unique reversible two-electron exchange on the time scale of the experiments. The latter step, involving two overlapping electron transfers, involves two independent redox centres. Spectroelectrochemical studies confirm that all electron transfers are ligand-centred and that the species generated are stable on the time scale of the spectroelectrochemical measurements, namely for at least 30 min, except for the species generated by the fourth oxidation. This tetracation generated undergoes further chemical reaction(s) and renders the fourth oxidation irreversible on the spectroelectrochemical time scale.

The present study also demonstrates that cyclooctaphyrins with (4*n* + 2) π-electrons possess more homogeneous electrochemical and spectral characteristics, whereas cyclooctaphyrins with 4*n* π-electrons exhibit a greater spread in the redox potentials and UV/Vis absorbance bands. The spectra of the species with (4*n* + 2) π-electrons exhibit an intense and sharp absorbance band, clearly resulting from an intense conjugation in the ligand.

Further studies are under way, especially on cyclooctaphyrins containing electroactive metals that are, up to now, rather scarce. Also, more insight into these new classes of compounds will be provided by theoretical approaches.

Experimental Section

General: All of the presently studied cyclooctapyrroles were, for reasons of solubility, employed as hexadecaethyl derivatives. The synthesis of compound **1**, namely 2,3,6,7,11,12,15,16,20,21,24,25,29,30,33,34-hexadecaethylcyclooctapyrrol-(1.0.1.0.1.0.1.0), and for species **2**, namely 2,3,7,8,12,13,16,17,21,22,26,27,31,32,35,36-hexadecaethylcyclooctapyrrol-(1.1.1.0.1.1.1.0), and **3**, namely 2,3,6,7,11,12,17,18,22,23,26,27,31,32,37,38-hexadecaethylcyclooctapyrrol-(2.1.0.1.0.2.1.0.1), have been published previously.[10,11] The figure-eight conformation confers two coordination sites on these molecules, and it has been shown that **1** and **2** are able to coordinate diverse transition metal ions to afford complexes of all three types, namely mononuclear, homo- and hetero-dinuclear complexes according to classical procedures.[19,20] Ligand **3** gave only some homodinuclear complexes according to published procedures.[20,21] The electrochemical measurements were carried out in a glove box (less than 3 ppm of H_2O and less than 2 ppm of O_2) at room temperature (25±2 °C) in PhCN containing 0.1 M Bu_4NPF_6 in a classical three-electrode cell. The electrochemical cell was con-

nected to a computerised multipurpose electrochemical device (PAR 273) interfaced with a PC computer. The working electrode was a platinum (Pt) disc electrode (diameter: 2 mm) used either motionless for cyclic voltammetry (v = 20 mV/s to 5 V/s) or as a rotating disc electrode. The auxiliary electrode was a platinum wire, and the pseudo-reference electrode was also a platinum wire. All potentials are referred to the ferrocenenium/ferrocene (Fc^+/Fc) couple used as an internal standard. Benzonitrile (PhCN, Aldrich, 99%) was dried, before use, for 2 d with $CaCl_2$ (anhydrous, Fluka, 97%), and distilled from P_2O_5 (Prolabo) under reduced pressure and argon. The main fraction was collected under argon and transferred into the glove box. The supporting electrolyte, Bu_4NPF_6 (Fluka − electrochemical grade) was dried in an oven (65 °C) under vacuum for 2 d. Bu_4NPF_6 was solubilised in PhCN inside the glove box and the solution was then percolated over activated aluminia. The available potentials on a platinum working electrode ranged from −2.5 to +1.8 V/Fc. Spectroelectrochemical measurements were carried out in PhCN in a home-made quartz cell, having an optical pathway of 1 mm. The working electrode was a platinum grid (1000 mesh) placed in the optical pathway. The reference and the auxiliary electrodes were platinum wires in individual compartments, separated from the solution by cotton. The cell was filled in the glove box, and hermetically closed, it was then placed in a diode array spectrophotometer (Hewlett−Packard 8453) and spectra were recorded during electrolysis. UV/Vis spectra were recorded in CH_2Cl_2 (Merck, spectroscopy grade, used as received) with a Varian Cary 05E UV/Vis/NIR spectrophotometer, at room temperature.

Acknowledgments

We are much indebted to the Ministère de la Recherche for a research fellowship to J. B. E. and to CNRS for financial and human resources.

[1] R. B. Woodward, in: *Aromaticity: an International Symposium*, Sheffield, UK, **1966**; special publication no. 21, The Chemical Society, London, **1966**.
[2] V. J. Bauer, D. L. J. Clive, D. Dophin, J. B. Paine, F. L. Harris, M. M. King, J. Loder, S. W. C. Wang, R. B. Woodward, *J. Am. Chem. Soc.* **1983**, *105*, 6429.
[3] M. J. Broadhurst, R. J. Grigg, A. W. Johnson, *J. Chem. Soc., Perkin Trans. 1* **1972**, 2111−2116.
[4] H. Rexhausen, A. Gossauer, *J. Chem. Soc., Chem. Commun.* **1983**, 275.
[5] A. Gossauer, *Bull. Soc. Chim. Belg.* **1983**, *92*, 793.
[6] R. Charrière, T. A. Jenny, H. Rexhausen, A. Gossauer, *Heterocycles.* **1993**, *36*, 1561.
[7] J. L. Sessler, T. Morishima, V. Lynch, *Angew. Chem. Int. Ed. Engl.* **1991**, *30*, 977−980.
[8] J. L. Sessler, S. J. Weghorn, T. Morishima, M. Rosingana, V. Lynch, V. Lee, *J. Am. Chem. Soc.* **1992**, *114*, 8306.
[9] J. L. Sessler, S. J. Weghorn, V. Lynch, M. R. Johnson, *Angew. Chem. Int. Ed. Engl.* **1994**, *33*, 1509−1512.
[10] M. Bröring, J. Jendrny, L. Zander, H. Schmickler, J. Lex, Y. D. Wu, M. Nendel, J. Chen, D. A. Plattner, K. N. Houk, E. Vogel, *Angew. Chem. Int. Ed. Engl.* **1995**, *34*, 2515−2517.
[11] E. Vogel, M. Bröring, J. Fink, D. Rosen, H. Schmickler, J. Lex, K. W. K. Chan, Y. D. Wu, D. A. Plattner, M. Nendel, K. N. Houk, *Angew. Chem. Int. Ed. Engl.* **1995**, *34*, 2511−2514.
[12] J. L. Sessler, D. Seidel, V. Lynch, *J. Am. Chem. Soc.* **1999**, *121*, 11257−11258.
[13] J. Setsune, Y. Katakami, N. Iizuna, *J. Am. Chem. Soc.* **1999**, *121*, 8957−8958.
[14] J. A. Wytko, M. Michels, L. Zander, J. Lex, H. Schmickler, E. Vogel, *J. Org. Chem.* **2000**, *65*, 8709−8714.
[15] T. D. Lash, *Angew. Chem. Int. Ed.* **2000**, *39*, 1763−1767.
[16] A. Jasat, D. Dolphin, *Chem. Rev.* **1997**, *97*, 2267−2340
[17] M. Shionoya, H. Furuta, V. Lynch, A. Harriman, J. L. Sessler, *J. Am. Chem. Soc.* **1992**, *114*, 5714.
[18] M. Gosmann, B. Franck, *Angew. Chem. Int. Ed. Engl.* **1986**, *25*, 1100−1101.
[19] L. Zander, PhD dissertation, Universität zu Köln, **1998**.
[20] M. Michels, PhD dissertation, Universität zu Köln, **1999**.
[21] A. Werner, M. Michels, L. Zander, J. Lex, E. Vogel, *Angew. Chem. Int. Ed.* **1999**, *38*, 3650−3653.
[22] J. P. Gisselbrecht, J. Bley-Escrich, M. Gross, L. Zander, M. Michels, E. Vogel, *J. Electroanal. Chem.* **1999**, *469*, 170−175.
[23] J. Tomeš, *Collect. Czech. Chem. Commun.* **1937**, *9*, 150.
[24] R. S. Nicholson, I. Shain, *Anal. Chem.* **1964**, *36*, 706−723.
[25] M. Rudolph, D. P. Reddy, S. W. Feldberg, *Anal. Chem.* **1994**, *66*, 589A−600A.
[26] F. Ammar, J. M. Savéant, *J. Electroanal. Chem.* **1973**, *47*, 215−221.
[27] R. L. Myers, I. Shain, *Anal. Chem.* **1969**, *41*, 980.
[28] D. H. Evans, M. W. Lehmann, *Acta Chem. Scand.* **1999**, *53*, 765−774.
[29] K. M. Kadish, *Prog. Inorg. Chem.* **1986**, *34*, 443.
[30] L. Guyard, P. Audebert, P. Hapiot, *J. Chem. Phys.* **1998**, *95*, 1192−1195.
[31] J. P. Gisselbrecht, M. Gross, E. Vogel, J. L. Sessler, *Inorg. Chem.* **2000**, *39*, 2850−2854.
[32] J. H. Fuhrhop, K. M. Kadish, D. G. Davis, *J. Am. Chem. Soc.* **1973**, *95*, 5140−5147.
[33] C. Bernard, J. P. Gisselbrecht, M. Gross, E. Vogel, M. Lausmann, *Inorg. Chem.* **1994**, *33*, 2393−2401.
[34] K. M. Barkigia, M. W. Renner, L. R. Furenlid, C. J. Medforth, K. M. Smith, J. Fajer, *J. Am. Chem. Soc.* **1993**, *115*, 3627−3635.
[35] J. P. Gisselbrecht, M. Gross, M. Köcher, M. Lausmann, E. Vogel, *J. Am. Chem. Soc.* **1990**, *112*, 8618−8620.
[36] C. Bernard. PhD dissertation, Université Louis Pasteur, Strasbourg, **1994**.
[37] M. W. Renner, A. Forman, W. Wu, C. K. Chang, J. Fajer, *J. Am. Chem. Soc.* **1989**, *111*, 8618−8621.
[38] C. Bernard, J. P. Gisselbrecht, M. Gross, N. Jux, E. Vogel, *J. Electroanal. Chem.* **1995**, *381*, 159−166.
[39] E. Hückel, *Z. Phys.* **1931**, *72*, 310.
[40] B. Franck, A. Nonn, *Angew. Chem. Int. Ed. Engl.* **1995**, *34*, 1795−1811.
[41] G. Märkl, T. Knott, P. Kreitmeier, T. Burgemeister, F. Kastner, *Helv. Chim. Acta* **1998**, *81*, 1480−1505.
[42] R. A. Berger, E. LeGoff, *Tetrahedron Lett.* **1978**, *44*, 4225−4228.
[43] J. L. Sessler, E. A. Bruker, S. J. Weghorn, M. Kisters, M. Schäfer, J. Lex, E. Vogel, *Angew. Chem. Int. Ed. Engl.* **1994**, *33*, 2308−2312.
[44] D. M. Guldi, P. Neta, A. Heger, E. Vogel, J. L. Sessler, *J. Phys. Chem.* **1998**, *102*, 960−967.
[45] H. J. Callot, A. Roher, T. Tschamber, B. Metz, *New J. Chem.* **1995**, *19*, 155−159.
[46] E. Vogel, M. Bröring, S. J. Weghorn, P. Scholz, R. Deponte, J. Lex, H. Schmickler, K. Schaffner, S. E. Braslavsky, M. Müller, S. Pörting, C. J. Fowler, J. L. Sessler, *Angew. Chem. Int. Ed. Engl.* **1997**, *36*, 1651−1654.
[47] J. L. Sessler, M. Cyr, A. K. Burrell, *Tetrahedron.* **1992**, *48*, 9661−9672.
[48] J. L. Sessler, M. J. Cyr, A. K. Burrell, *Synlett* **1991**, 127−134.
[49] J. L. Sessler, S. J. Weghorn. *Expanded, Contracted & Isomeric Porphyrins*, Elsevier Science Ltd., Redwood Books, Wiltshire, **1997**.
[50] J. L. Sessler, S. J. Weghorn, Y. Hiseada, V. Lynch, *Chem. Eur. J.* **1995**, *1*, 56−67.

Received March 12, 2002
[I02128]